Xe-C Scattering, Implantation, and Sputtering Analysis for EP Systems

IEPC-2024-552

Presented at the 38th International Electric Propulsion Conference
Pierre Baudis Convention Center • Toulouse, France
June 23-28, 2024

Luke K. Franz[1] and Richard E. Wirz[2]
Oregon State University, Corvallis, Oregon, 97333, U.S.A.

Electric propulsion facility effects are strongly influenced by the interaction of the ion beam with facility surfaces through processes such as ion scattering, implantation, and ejection, as well as sputtering of the impinged material. The ion-solid irradiation program, TRI3DYN, simulates the reflective scattering and post-implantation ejection of xenon from carbon at 300-, 600-, and 900-eV incidence. These energies are chosen to represent single-, double-, and triple-charged ions from a 300-volt Hall effect thruster or to approximate single-charged ions for higher voltage thruster operation. Outputs of carbon sputtering are compared against data from the literature as a means of model validation, which required adjustments to the surface binding energy scaling (SBES) and maximum atomic ratio of xenon-in-carbon implantation (EXST, EXcess Stoichiometry Treatment) parameters in TRI3DYN. Trajectories, energies, and yields of xenon scatterants, ejecta, and carbon sputterants are described for angles of incidence on amorphous carbon at 0°, 20°, 30°, 45°, 60°, 70°, and 80°. These dynamic models elucidate details about mass and energy transport for carbon materials in EP systems during plasma bombardment and provide a basis with which TRI3DYN can more accurately describe these interactions.

Nomenclature

SBES	=	Surface Binding Energy Scaling, TRI3DYN parameter
EXST	=	EXcess Stoichiometry Treatment, TRI3DYN parameter
CV	=	Control Volume
BC	=	Boundary Condition
VCM	=	Volumetrically Complex Material
Y	=	Particle yield [atoms/ion]
E	=	Average energy per particle [eV]
θ	=	Average outgoing angle or angle of emission [°]
X_{sp}, X_{sc}, X_{ej}	=	Generic variables in terms of sputterants, scatterants, or ejecta
PDF	=	Probability Distribution Function
Res	=	Voxel Resolution (cubic edge length, [μm])
ϕ	=	Angle of incidence [°]

[1]Graduate Student, Oregon Space Grant Consortium Fellow, College of Engineering, franzlu@oregonstate.edu
[2]Executive Director of Aerospace Research Programs, Boeing Professor, College of Engineering, Richard.Wirz@oregonstate.edu

I. Introduction

NOBLE gas ions emitted from electric propulsion (EP) thrusters become the primary source of neutral ingestion in ground tests and cause sputtering erosion of EP components due to plasma-material interactions (PMI).[1,2,3] This research objective is to model the mass and energy transport of xenon ions as they interact with rough carbon surfaces in EP systems. This paper analyses parameter selections in the ion-irradiation program, TRI3DYN, to simulate the xenon life cycle with amorphous carbon materials in addition to carbon sputtering.

Four types of PMI are studied herein: (1) *Scattering* – the reflection of an incident xenon ion off, or out of, the carbon surface. (2) *Implantation* – the insertion of an incident xenon ion into the carbon matrix. (3) *Sputtering* – the dislodging and emission of carbon atoms from the matrix due to energy transfer from the incident projectile. (4) *Ejection* – a form of sputtering which considers the ejection of implanted xenon atoms from the carbon matrix, hereby referred to as *ejecta* (see Fig. 1).

Complications with EP facility effects during ground tests and spacecraft lifetime concerns from sputter erosion motivate the effort to establish a computational environment in TRI3DYN that approximates an EP-relevant material system. TRI3DYN uses the binary collision approximation to simulate individual collision events between an incident projectile (xenon) and a voxelated amorphous material matrix (carbon) at random coordinates along the entire control volume (CV) surface. Using TRI3DYN's dynamic mode, material damages induced by collisions are saved to memory and are allowed to evolve during succeeding collisions. This dynamic capability facilitates the option to track the life cycle of incident species as they scatter, implant, or eject from the material throughout a pre-defined total fluence (number of incident projectiles over the entire material surface area). Using experimental carbon sputter yields as a metric for validation against these simulations, a combination of TRI3DYN input parameters result in yields that align with data from the literature. Outputs for scatterant, ejectant, and sputterant energies, directions, and yields are presented herein.

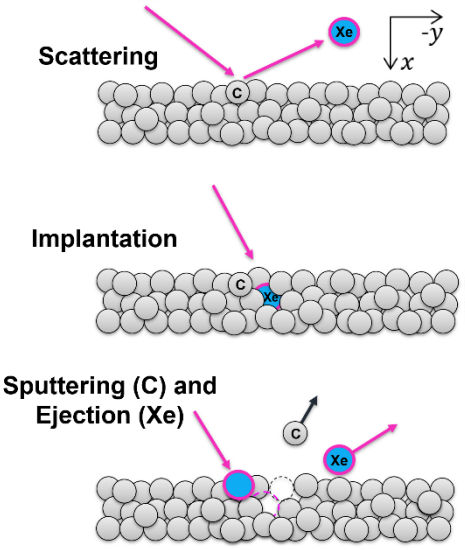

Figure 1: Visualization of the four modes of plasma-material interactions (PMI) that are simulated in this research.

II. Methods

A. Establishing the Simulation Environment

Required input parameters for TRI3DYN are first established which include the initial material geometry, total simulated fluence, material matrix overall dimensions, voxel dimensions (3D mesh grid), boundary conditions, and irradiation parameters (energy, angle of incidence). Table 1 shows the chosen mandatory simulation parameters followed by explanations for each parameter.

Table 1: TRI3DYN's mandatory parameter selections. *Some parameters are changed in specific analyses.

	Fluence						
Initial Material Geometry	**Pseudo-projectiles**	**Ions/ Pseudo-projectile**	**Material Dimensions [$\mu m, \mu m, \mu m$]**	**Voxel Dimensions* [$\mu m, \mu m, \mu m$]**	**Boundary Conditions**	**Incident Energy* [eV]**	**Angle of Incidence* (°)**
Flat, Semi-infinite	19.12E+06	14.54E+07	(20, 40, 40) x y z	(0.4, 0.4, 0.4) x y z	Periodic	300, 600, 900	0, 20, 30, 45, 60, 70, 80

The 38th International Electric Propulsion Conference, P. Baudis Convention Center, Toulouse, France June 23-28, 2024

The **initial material geometry** sets the coordinates of voxel positions prior to ion bombardment, which in this study composes a flat amorphous surface. In dynamic mode, this surface roughens from sputter erosion, and Fig. 3 shows that steady state yields can be approximated at the fluence explored. **Fluence** is chosen based on a first-order approximation of the average ion fluence after 50 hours on Georgia Institute of Technology's central beam target at a xenon feed rate of $10\,\frac{mg}{s}$. TRI3DYN automatically organizes groupings of incident ions to create *pseudoprojectiles*, which behave as normalized particle clusters for computational efficiency.[4]

Material dimensions define the CV size under irradiation. The irradiated surface area is set as $40\ \mu m$-by-$40\ \mu m$ with a depth of $20\ \mu m$. **Voxel dimensions** describe the discretized material mesh composed of three-dimensional cubic voxels with edge lengths of $0.4\ \mu m$. The default algorithm in TRI3DYN creates surface smoothing through an averaging process with first-, second-, then third-order nearest neighboring voxels.[4,5]

Boundary conditions (BC) are set as 'periodic' to emulate PMI on a larger scale (order of millimeters) than what is recorded in TRI3DYN (order of microns). A periodic BC relocates an atom that leaves one boundary edge back into the CV through the opposite edge. If periodic were not selected, the CV would be simulated as an isolated $3200\ \mu m^3$ plate as opposed to a differential piece of a larger part in an EP system.

Incident energies and angles are set to represent the largest practical range of those parameters experienced during thruster operation. At incident ion energies of 300, 600, and $900\ eV$, projectile particles emulate the energy of single-, double-, and triple-charged ions from a 300-V Hall effect thruster, or approximate single-charged ions for higher voltage operation. The chosen angles of incidence offer PMI outputs for a wide range of potential EP system orientations. Indeed, efforts toward the design and optimization of EP system orientations and geometries are being pursued with attention to the beam target, along with volumetrically complex materials (VCMs), in the Plasma, Energy, and Space Propulsion Laboratory (PESPL).[6,7,20]

B. EXST & SBES Parameter Sweep

By default, TRI3DYN's 'static mode' erases material damage information caused by a projectile before the succeeding projectile is simulated. As a result, information about the life cycle of xenon projectiles is erased. By using TRI3DYN's memory capabilities in 'dynamic mode,' the life cycle of Xe-C irradiation is explored herein.

As a default phenomenon in TRI3YDN, implanted xenon atoms are permitted to completely fill a voxel's mass. At the plasma conditions for the EP systems considered, xenon should not act as a solid, therefore, TRI3DYN's Xe-implantation-limit parameter, EXST (EXcess Stoichiometry Treatment), limits the amount of xenon permitted in a voxel of carbon atoms. When a voxel's atomic fraction of xenon exceeds EXST, those atoms are programmed to diffuse to the nearest unsaturated voxel. An initial approximation for EXST is made based on a hypothetical unit crystal cell of graphite containing a xenon atom defect. If a xenon atom were present in one unit cell of graphite, the induced stress field might prevent a neighboring unit cell from hosting a xenon atom defect. Assuming one xenon atom per two graphite unit cells (1 unit cell of graphite = 4 carbon atoms), the initial value of EXST is set to 0.125. EXST = 0.5 is used as a second comparison value to observe what happens in an extreme case.

TRI3DYN also offers an optional SBES (Surface Binding Energy Scaling) parameter which is varied in the same study (section E) to observe the relative impacts of each parameter on sputter and ejection yield (Y_{sp} and Y_{ej}, respectively) and probability distribution function (PDF) results.

After the results from the EXST and SBES sweep have been compared to the literature, another parameter sweep on EXST results in simulated sputter yields within a range of likelihood bounds, modeled by Tran and Chew, which fit well with empirical data.[8] The limits of the EXST sweep were chosen according to experiments that measured the concentration of xenon in amorphous carbon materials after irradiation exposure to be between 10 and 14%.[9,10] Simulated data points for angle- and energy-dependent carbon sputter yields are plotted from normal to glancing incident angles for two incident energies to examine TRI3DYN's sputter yield profile.

C. Surface Roughness Sensitivity Analysis

A voxel resolution (Res) of $0.4\ \mu m$ was initially chosen based on approximating the surface roughness of considerably smooth graphite parts, wherein one change in voxel depth represents one unit of the estimated surface roughness. To address the uncertainty with this surface roughness estimation, a brief sensitivity analysis on the resolution selection was performed between Res = 0.4 and 0.2 (see section F).

This sensitivity analysis compares Y_{sp} vs. ϕ at normal 300-eV xenon incidence in either resolution. Probability distribution functions of scatterants and ejecta are plotted for 0° and 70° incidence to compare the differences in average scattering and ejection angles of emission from the roughened surfaces.

The 38th International Electric Propulsion Conference, P. Baudis Convention Center, Toulouse, France June 23-28, 2024

D. Data Collection for Scatterants, Ejecta, and Sputterants

Once each parameter under consideration has been analyzed and decisions for each have been determined, final outputs are presented for yields, average outgoing energies per particle, and average angles of emission for xenon scatterants, xenon ejecta, and carbon sputterants (see Fig. 6-9).

III. Results

E. SBES and EXST Parameter Sweeps

By changing either SBES or EXST at one time, the impacts of each parameter on the properties of sputtered and ejected species can be realized through PDFs (Fig. 2) and yield profiles (Fig. 3). One of the implications of increasing EXST or SBES is a decrease in the carbon sputter yield due to a lower proportion of the CV being composed of carbon (in the case of EXST) or the material bonds being difficult to break (in the case of SBES). This decrease in carbon yield is explicitly presented in Fig. 3 and can be interpreted from Fig. 2.

By comparing the top row to the bottom row of Fig. 2, one will notice a larger proportion of xenon being ejected in the bottom row by how the total sputter PDF (sputterants + ejecta) approaches the ejectant (Xe) PDF. The left column to the right column of the same figure represents a sweep over a lower and higher surface binding energy scaling factor, respectively. Because more energy is required to break carbon bonds in the right column cases, less carbon is sputtered, and therefore, the sputterant (C) PDF is more jagged in the right column due to there being fewer data points to contribute toward the gaussian smoothing filter (sigma = 3).

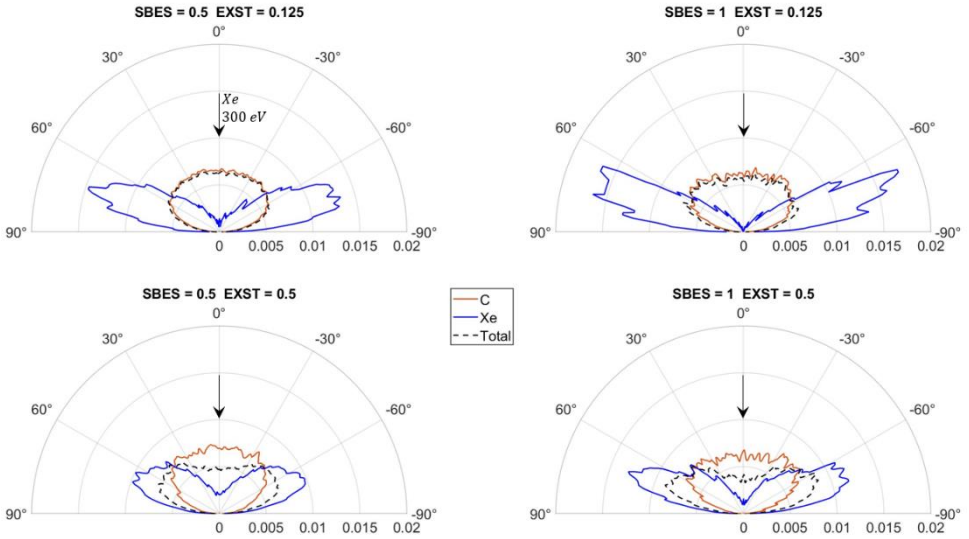

Figure 2: Sputterant (C) and Ejectant (Xe) Probability Distribution Functions. Sputtering and ejection trajectories, presented as PDFs, result from an SBES (left to right) and EXST (top to bottom) parameter sweep from 0°, 300-eV, Xe-C irradiation. Carbon sputter yields are in orange, xenon ejecta in blue, and total (C + Xe) in black dash. Each species-differentiated PDF (Xe, C, or total) individually sum to unity.

Fig. 3 displays yield plots for sputterants and ejecta, highlighting the steady state carbon sputter yields as dashed horizontal lines. A parameter combination of EXST = 0.125 and SBES = 0.5 is shown to align with a range of experimental carbon sputter yields. Tran and Chew's MD results suggest that various allotropes of carbon quickly become amorphized in plasma energy regimes like those explored herein,[8] which supports the argument that TRI3DYN's amorphous model may be related to various experiments that use different carbon allotropes. An additional parameter sweep is performed in Fig. 4 to refine the implantation parameter, EXST, around a range of values measured in experiment (10%-15%).[9,10] To validate the TRI3DYN model, angle- and energy-dependent sputter yields are compared with the literature, and an implantation limit of 15% xenon-in-carbon resulted in sputter yields within a range of likelihood bounds[8] at four angles of incidence ($0°, 30°, 45°, 60°$) from two different xenon incident energies (300 and 400 eV).

The 38th International Electric Propulsion Conference, P. Baudis Convention Center, Toulouse, France June 23-28, 2024

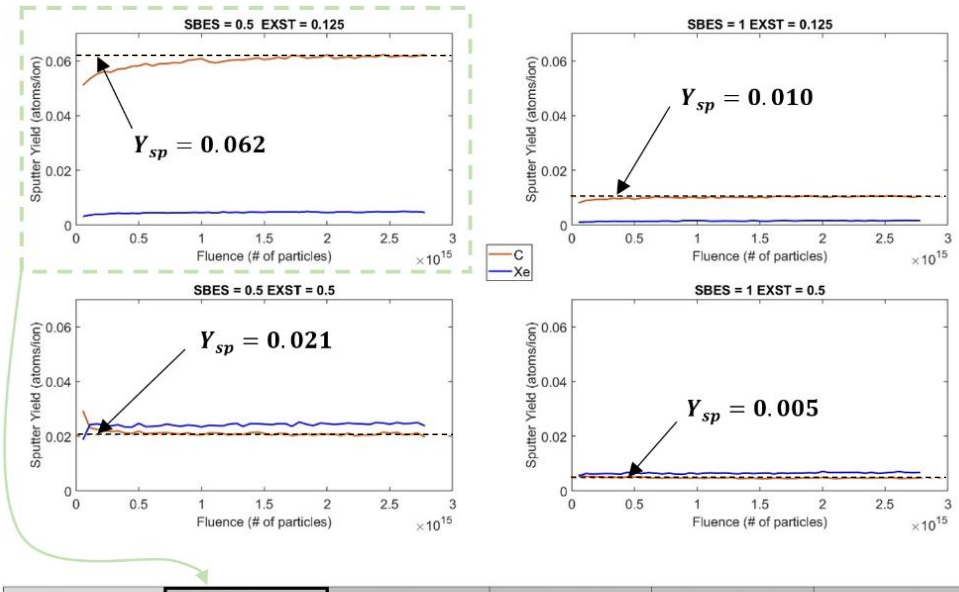

Source	TRI3DYN, EXST=0.125 SBES=0.5	[11]C-C Composite	[11]Pyrolytic Graphite	[12]Pyrolytic Graphite	[13]Amorphous Carbon
Sputter Yield, Y_{sp} [atoms/ion]	**0.062**	0.046	0.050	0.080	0.124±0.029

Figure 3: Sputter (C) and Ejecta (Xe) Yields vs. Fluence. Steady state carbon sputter yields for each parameter combination in the EXST-SBES analysis are represented as dashed lines and are labeled as Y_{sp} in the plots. A table is provided to show the [SBES=0.5 EXST=0.125] case outputting a sputter yield within a range of four experimental measurements.

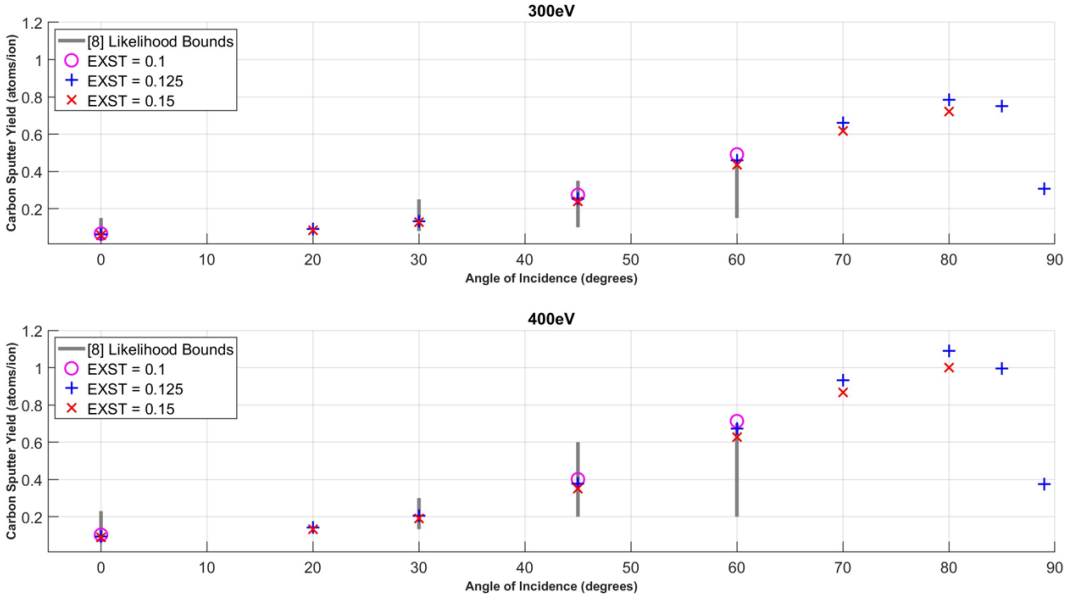

Figure 4: Sputter Yield vs. Angle of Incidence; EXST Parameter Refinement. Sputter yields are plotted against angles of normal to glancing incidence at xenon energies of 300 and 400 eV. Vertical gray lines represent likelihood bounds from Tran and Chew, which align well with empirical data.[8] TRI3DYN data is separated into three markers, each representing different EXST parameter selections. EXST = 0.15 outputs sputter yields within the likelihood bounds at four different incident angles under both incident energies. This corroborates the finding that around 14% xenon is implanted in amorphous carbon under plasma conditions like those explored in this research.[10]

F. Mesh Resolution Sensitivity

Using SBES = 0.5 and EXST = 0.15 as the case that aligns closest with the literature, a final analysis is performed on the CV mesh resolution. Fig. 5 presents results on steady state carbon sputter yields from normal 300-eV incidence using two resolutions, along with scatterant and ejectant PDFs from 0° and 70° incidence with the same 300-eV incident energy. PDFs are used to compare the average angles of emission (represented as hexagrams) from 70° incidence between the two resolution cases.

Steady state carbon yields are shown to differ by 4% while the average outgoing angles of ejecta differ by 3°. It should be noted that differences across simulation outputs are to be expected, even under identical parameter selections, because of TRI3DYN's randomized Monte Carlo algorithm.

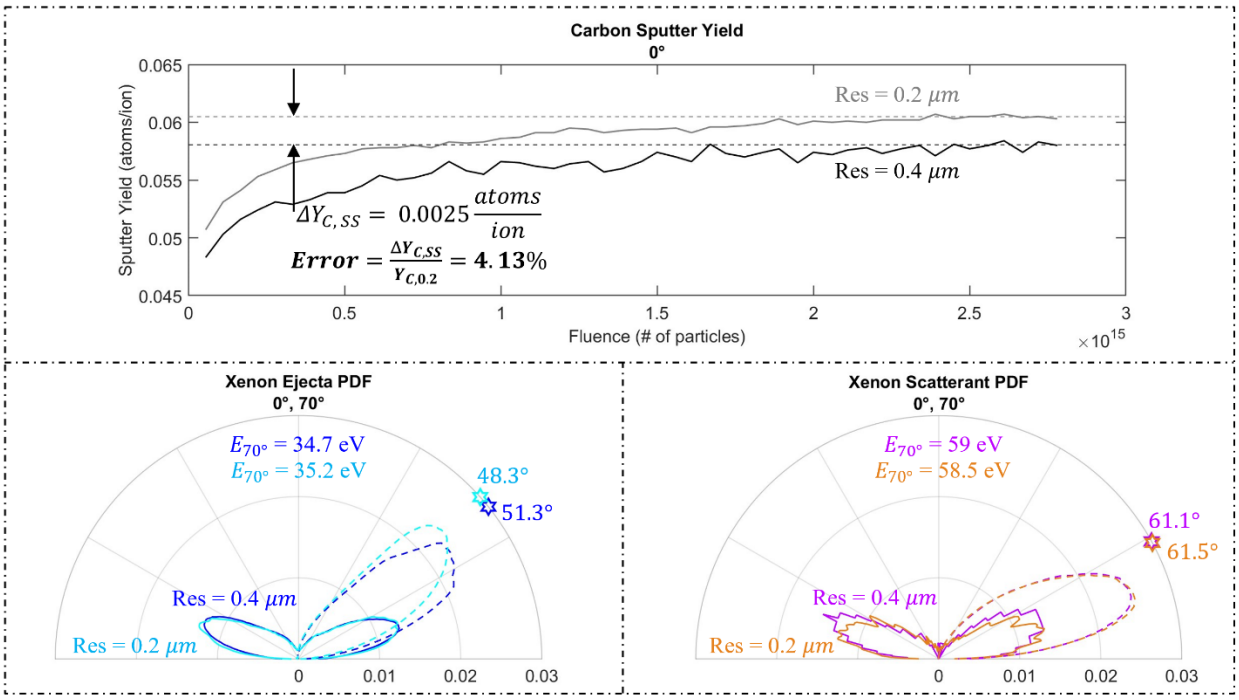

Figure 5: Sensitivity analysis between 0.2-μm and 0.4-μm voxel edge lengths (Res = [0.2 0.4]). Carbon sputter yield is shown to increase by 4.13% at higher voxel resolution while xenon ejects from the carbon matrix 3° shallower, on average, than the lower resolution case during 70° xenon bombardment. The variance between these metrics due to the random Monte Carlo algorithm of TRI3DYN also contributes to differences between simulations.

G. Energy and Mass Transport of Scatterants, Ejecta, and Sputterants

With each parameter used in this TRI3DYN study having been analyzed, final outputs are presented in Fig. 6-9. Figures 7-9 present average energies, yields, and outgoing angles for scatterants, ejecta, and sputterants at normal to glancing angles with 300-, 600-, and 900-eV incidence, while Fig. 6 summarizes the energies and emission angles of each species along with their PDFs.

Such data informs predictive engineering models and experimental sputter deposition analyses of particle contaminant transportation in EP vacuum testing facilities.[14-17] Reducing EP testing uncertainties from facility effects can be achieved by developing models for contaminant species (i.e., scatterants, ejecta, and sputterants) to predict their behavior and account for their contributions to thruster operation.[6,7,14-17] The physics-informed particle transport results in Fig. 6-9 provides data for such efforts taking place in the Plasma, Energy, and Space Propulsion Laboratory, with emphasis on reducing chamber background pressure, tracking sputter flux toward thrusters under testing, and applications to EP system design and optimization for PMI management.[6,7,18-20]

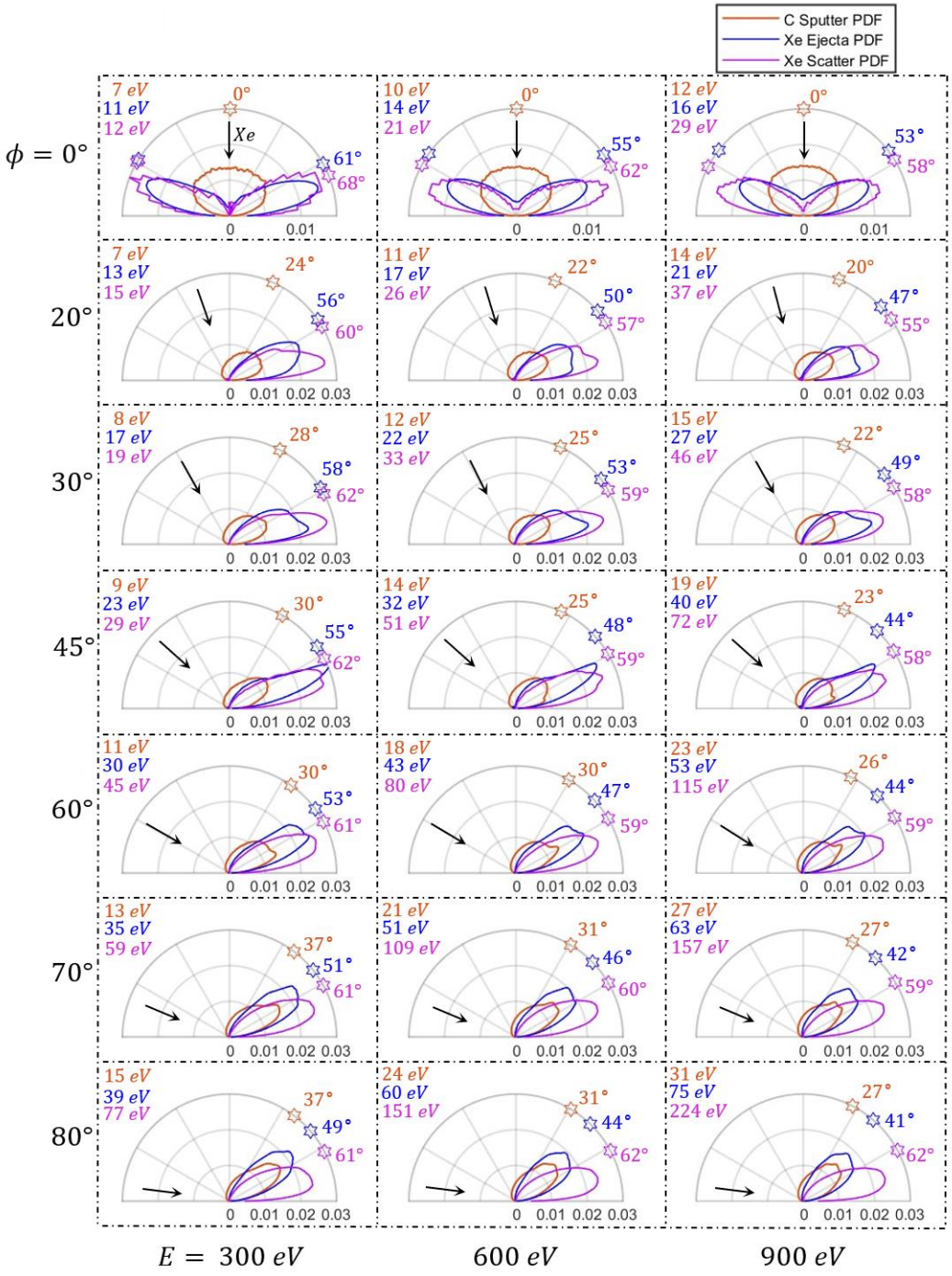

Figure 6: Probability Distributions Functions for Ejecta (blue), Scatterants (pink), and Sputterants (orange). Incident xenon is portrayed as a black arrow for normal to glancing angles at 300, 600, and 900 eV. Average energies per particle are given in the top left of each subplot, and average outgoing angles are shown next to their respective markers along polar plot edges. At normal angles of incidence, only the forward-scattered and -ejected angles are labeled due to symmetry about the surface normal. Smoother PDFs are observed with larger datasets, or, in cases with higher yields (see Fig. 8).

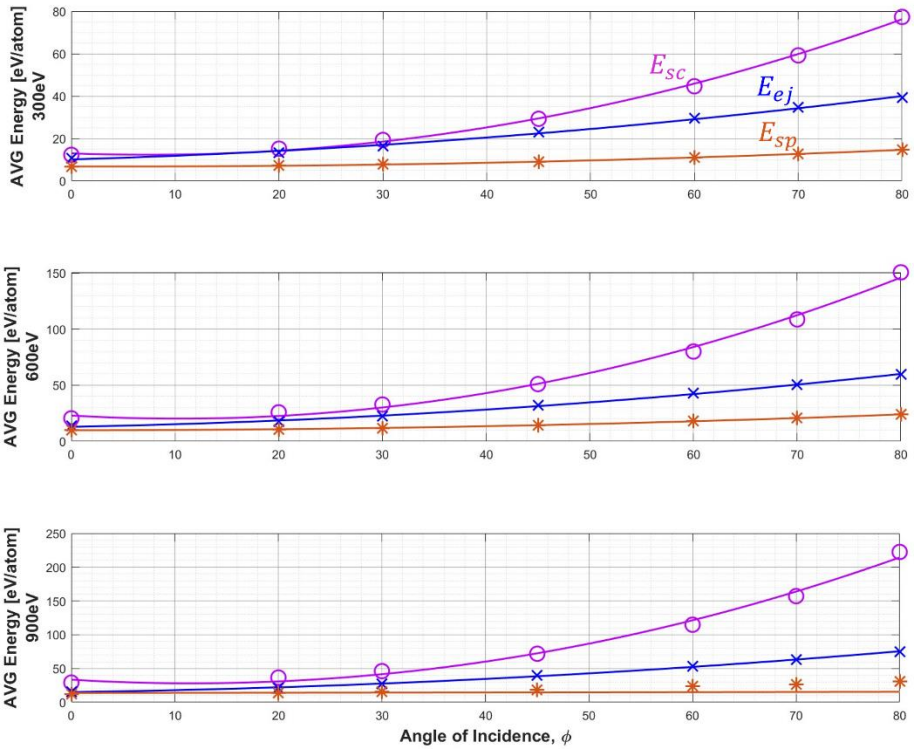

Figure 7: Average Energy per Ejectant (blue), Scatterant (pink), and Sputterant (orange) vs. Angle of Incidence. Scatterants are shown to retain the most energy at glancing angles of incidence.

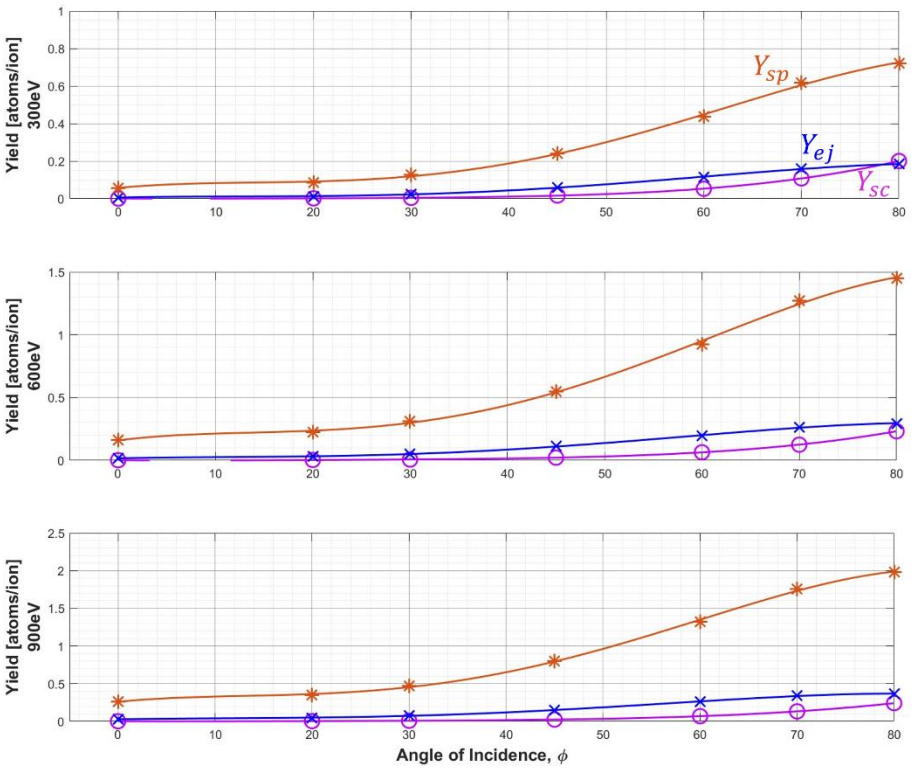

Figure 8: Yields of Ejecta, Scatterants, and Sputterants vs. Angle of Incidence. Carbon sputterants are shown to compose most of the emitted species at high angles of incidence.

While Fig. 7-8 may be used to calculate total energy flux of a given species from bombardment of a certain incident energy and angle, Fig. 9 offers insight into which direction these species are likely to emit at those conditions. Regardless of the angle of incidence, all species tend to emit within a 20° range, with the most variance seen among carbon sputterants.

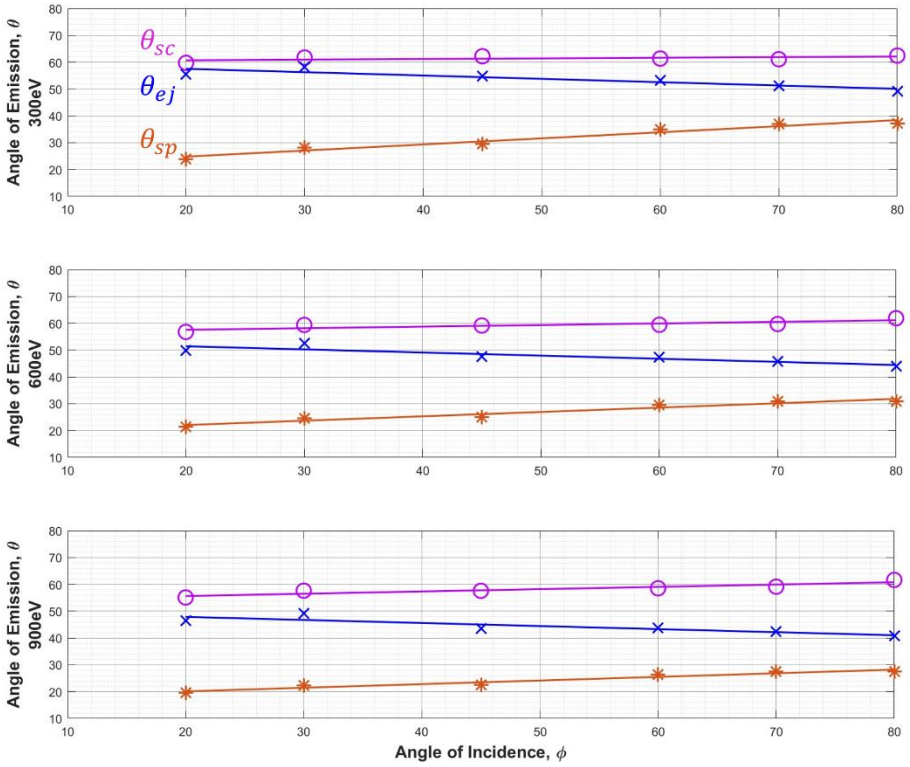

Figure 9: Average Emission Angle of Ejecta, Scatterants, and Sputterants vs. Angle of Incidence, measured in degrees.

IV. Conclusions & Future Work

The ion-solid irradiation program, TRI3DYN, was used to simulate xenon and carbon behavior during bombardment of amorphous carbon with consideration of the plasma conditions experienced in EP systems. A series of parameter sweeps on the implantation limit of xenon-in-carbon (EXST), surface binding energy scaling (SBES), and voxel resolution (Res) were performed to analyze their impacts on outputs of scatterant, ejectant, and sputterant energies, angles of emission, and yields. A maximum atomic ratio of 15% xenon-in-carbon, along with a surface binding energy scaling factor, resulted in carbon sputter yields that are corroborated by data from the literature. Using a validated set of parameters, outputs for PDFs, average energies per particle, average angles of emission, and yields of each species at normal to glancing angles of incidence for 300-, 600-, and 900-eV incident xenon ions were provided. Scatterants retain around 25% of their energy at 80° incidence with 20% yield. Ejecta also exhibit 20% yield at near-grazing incidence, however, their average outgoing energies are around 10% of their incidence energy. Regardless of incidence angle, all species are emitted within a 20° range, with scatterants being the most consistent at average outgoing angles between 55° and 62°.

Current efforts in the Plasma, Energy, and Space Propulsion Laboratory at Oregon State University incorporate TRI3DYN results to model particle movement across EP system boundaries. Applications include beam target optimization, volumetrically complex material (VCM) design, and chamber optimization for PMI management.[6,7,20] Using this research methodology, xenon life cycle modeling extends beyond reflected particles and includes post-implanted ejecta. Future work seeks to experimentally validate each emitted species' trajectory.

Acknowledgments

The authors offer sincere appreciation to lab mates Graeme Sabiston, Richard A. Obenchain, and Ehsan Taghizadeh for their generous time and support with this research, in addition to Oregon State University Professors Dr. Santala, Dr. Wildenschild, and Dr. Xu. This work was supported in part through NASA and Oregon Space Grant Consortium, cooperative agreement 80NSSC20M0035n, and the Joint AdvaNced PropUlsion InStitute, 20-STRI-FULL-0004, NASA Grant Number 80NSSC21K1118.

References

[1]Ito, Gen, Rei Kawashima, Kimiya Komurasaki, and Hiroyuki Koizumi. "Method of Suppressing Ingestion Particles Flowing Back to a Hall Thruster Using a Beam Target during Ground Testing." *TRANSACTIONS OF THE JAPAN SOCIETY FOR AERONAUTICAL AND SPACE SCIENCES* 65, no. 4 (2022): 160–71. https://doi.org/10.2322/tjsass.65.160.

[2]Tartz, M., E. Hartmann, R. Deltschew, and H. Neumann. "Experimental Validation of a Grid Erosion Simulation." In *35th Joint Propulsion Conference and Exhibit*. Los Angeles, CA, U.S.A.: American Institute of Aeronautics and Astronautics, 1999. https://doi.org/10.2514/6.1999-2860.

[3]Obenchain, Richard A., and Richard E. Wirz. "Neutral Ingestion Compensation for Gridded Ion Thrusters via Model Analysis." Boston, 2024.

[4]Möller, Wolfhard. "TRI3DYN – Collisional Computer Simulation of the Dynamic Evolution of 3-Dimensional Nanostructures under Ion Irradiation." *Nuclear Instruments and Methods in Physics Research Section B: Beam Interactions with Materials and Atoms* 322 (March 2014): 23–33. https://doi.org/10.1016/j.nimb.2013.12.027.

[5]Möller, Wolfhard. "TRI3DYN_2022 User Guide." HZDR, 2022.

[6]Franz, L., "Optimizing Beam Targets for Spacecraft Electric Propulsion," Online, May 2024, Oregon NASA Space Grant Consortium Spring 2024 Symposium

[7]Sabiston, Graeme. "Electric Propulsion Vacuum Chamber Design Approaches for Reducing Sputtering Effects." International Electric Propulsion Conference. Toulouse, France, 2024.

[8]Tran, H., and H.B. Chew. "Surface Morphology and Carbon Structure Effects on Sputtering: Bridging Scales between Molecular Dynamics Simulations and Experiments." *Carbon* 205 (March 2023): 180–93. https://doi.org/10.1016/j.carbon.2023.01.015.

[9]Marques, F.C., P.F. Barbieri, G.A. Viana, and D.S. da Silva. "Implantation of Xenon in Amorphous Carbon and Silicon for Brachytherapy Application." Applied Surface Science 275 (2013).

[10]Doerner, R. P., D. G. Whyte, and D. M. Goebel. "Sputtering Yield Measurements during Low Energy Xenon Plasma Bombardment." Journal of Applied Physics 93, no. 9 (n.d.).

[11]Williams, John D., Mark L. Johnson, and Desiree D. Williams. "Differential Sputtering Behavior of Pyrolytic Graphite and Carbon-Carbon Composite Under Xenon Bombardment." American Institute of Aeronautics and Astronautics, n.d.

[12]Rosenberg, D., and G. K. Wehner. "Sputtering Yields for Low Energy He+-, Kr+-, and Xe+-Ion Bombardment." Journal of Applied Physics 33, no. 5 (May 1, 1962): 1842–45. https://doi.org/10.1063/1.1728843.

[13]Kolasinski, Robert D., James E. Polk, Dan Goebel, and Lee K. Johnson. "Carbon Sputtering Yield Measurements at Grazing Incidence." *Applied Surface Science* 254, no. 8 (February 2008): 2506–15. https://doi.org/10.1016/j.apsusc.2007.09.082.

[14]Wirz, R. E. et al. "Predictive Engineering Model for Life and Performance Assessment of High-Power Electric Propulsion Systems," 37th International Electric Propulsion Conference, 2022, pp. IEPC–2022–410

[15]Cretel, C. M., Wirz, R. E. "Ion Thruster Grid Life and Performance Assessment via Reduced Order Modeling," 38th International Electric Propulsion Conference, 2024, pp. IEPC–2024–758

[16]Cowan, R. W., Biswas, S., Franz, L. K., Cretel, C. M., Obenchain, R. A., Wirz, R. E. "Hall Thruster Krypton Sputtering Effects on Vacuum Facility Materials," 38th International Electric Propulsion Conference, 2024, pp. IEPC–2024–549

[17]Biswas, S., Obenchain, R. A., Cowan, R. W., Wirz, R. E. "Review of PMI Data for HET-Induced Erosion of Facility Surfaces," 38th International Electric Propulsion Conference, 2024, pp. IEPC–2024–532

[18]Wirz, R. E. et al. "Electric Propulsion Research Activities in the Plasma, Energy, and Space Propulsion Laboratory," 38th International Electric Propulsion Conference, 2024, pp. IEPC–2024–802

[19]Taghizadeh, E., Obenchain, R. A., Franz, L. K. "Reduced Order Modeling and Optimization for EP Vacuum Chambers," 38th International Electric Propulsion Conference, 2024, pp. IEPC–2024–588

[20]Sabiston, Graeme, and Wirz, Richard E. "Ion-Surface Interactions in Plasma-Facing Material Design." *Journal of Applied Physics* 135, no. 18 (May 14, 2024): 183301. https://doi.org/10.1063/5.0201758